

Inference for reaction networks using the Linear Noise Approximation

Paul Fearnhead^{1,*}, Vasileios Giagos^{2,**}, and Chris Sherlock^{1,***}

¹Department of Mathematics and Statistics, Lancaster University, Lancaster, LA1 4YF, UK.

²School of Mathematics, Statistics and Actuarial Science, University of Kent, Canterbury, Kent CT2 7NF, UK.

**email*: p.fearnhead@lancaster.ac.uk

***email*: v.giagos@kent.ac.uk

****email*: c.sherlock@lancaster.ac.uk

SUMMARY: We consider inference for the reaction rates in discretely observed networks such as those found in models for systems biology, population ecology and epidemics. Most such networks are neither slow enough nor small enough for inference via the true state-dependent Markov jump process to be feasible. Typically, inference is conducted by approximating the dynamics through an ordinary differential equation (ODE), or a stochastic differential equation (SDE). The former ignores the stochasticity in the true model, and can lead to inaccurate inferences. The latter is more accurate but is harder to implement as the transition density of the SDE model is generally unknown. The Linear Noise Approximation (LNA) arises from a first order Taylor expansion of the approximating SDE about a deterministic solution and can be viewed as a compromise between the ODE and SDE models. It is a stochastic model, but discrete time transition probabilities for the LNA are available through the solution of a series of ordinary differential equations. We describe how a restarting LNA can be efficiently used to perform inference for a general class of reaction networks; evaluate the accuracy of such an approach; and show how and when this approach is either statistically or computationally more efficient than ODE or SDE methods. We apply the LNA to analyse Google Flu Trends data from the North and South Islands of New Zealand, and are able to obtain more accurate short-term forecasts of new flu cases than another recently proposed method, although at a greater computational cost.

KEY WORDS: Linear Noise Approximation; Reaction network; Google Flu Trends.

1. Introduction

Reaction networks are used to model a wide variety of real-world phenomena; they describe a probabilistic mechanism for the joint evolution of one or more populations of *species*. These *species* may be biological species, such as a range of different proteins (e.g. [Golightly and Wilkinson, 2005, 2008](#); [Boys et al., 2008](#); [Ferm et al., 2008](#); [Proctor et al., 2005](#)), animal species, such as predators and their prey (e.g. [Boys et al., 2008](#); [Ferm et al., 2008](#)), or interacting groups of humans or animals such as those infected with a particular disease, those susceptible to the disease and those who have recovered from it (e.g. [Andersson and Britton, 2000](#); [Ball and Neal, 2008](#); [Jewell et al., 2009](#)).

The evolution of these networks is most naturally modelled via a continuous-time jump Markov process. The current *state* of the system is encapsulated in a vector giving the numbers of each species that are present. The evolution of the state is described by a series of *reactions*, such as the interaction of two copies of a protein producing a dimer of that protein; or an interaction between an infected individual and a susceptible individual resulting in the susceptible becoming infected. Occurrences of a given reaction are modelled as a Poisson process, the rate of which depends on the current state of the system. Interest lies in inferring the parameters that govern the rate of each reaction from data on the evolution of the system.

This article concerns inference for the rate parameters and prediction of the future state in discretely observed reaction networks allowing that observations may contain noise and may be of only a subset of the species in the system. Inference under the jump Markov process is possible only for networks which involve few species, few reactions, and not “too many” transitions between observations (e.g. [Boys et al., 2008](#); [Amrein and Künsch, 2012](#)). For most systems it is necessary to approximate the evolution of the process to make inference computationally feasible. Often this will involve approximating the evolution through a system of ordinary differential equations (ODEs, e.g. [Jones et al., 2010](#)) or stochastic differential

equations (SDEs, e.g. [Wilkinson, 2006](#)). Models based on ODEs are only appropriate for very large systems for which the stochasticity in the evolution is small. For medium-size systems [Wilkinson \(2006\)](#) shows that SDE models are more appropriate and can lead to sensible estimates of the reaction rates. However inference for SDE models is non-trivial, as the transition density of general SDEs is unknown.

In this paper we use an alternative approximation, known as the Linear Noise Approximation (LNA) ([van Kampen, 1997](#); [Elf and Ehrenberg, 2003](#); [Hayot and Jayaprakash, 2004](#); [Ferm et al., 2008](#)). The LNA is obtained through first approximating the dynamics by a system of ODEs, and then modelling the evolution of the state about the deterministic solution of the ODE, through a linear SDE. Simulations suggest that this approach has similar accuracy to modelling the system directly through SDEs, but it has the important advantage that under the LNA the stochastic model for the states is a Gaussian process. Transition densities are therefore Gaussian, and their mean and covariance can be obtained through solving a system of differential equations. Using the LNA can therefore be more accurate than modelling the system via ODEs, and it is substantially easier to perform inference than under a general SDE model.

The structure of the paper is as follows. The next section provides more information on reaction networks and details two particular examples that will be revisited: the Lotka-Volterra predator-prey system, and an autoregulatory gene network. [Section 3](#) examines the different possible approximations to the evolution of reaction networks: ODE approximation; SDE approximation and the LNA. [Section 4](#) shows how we can calculate likelihoods using a ‘restarting’ LNA for a range of observation models, and suggests a simple way of embedding this within MCMC to perform Bayesian inference. We evaluate the use of the LNA empirically on both simulated and real data. An alternative use of a (non-restarting) LNA for inference on reaction networks has previously been suggested by [Komorowski et al. \(2009\)](#).

In Section 5 we compare our approach with that of Komorowski et al. (2009), with the simple ODE approximation, and with the SDE-based algorithm of Golightly and Wilkinson (2005). In Section 6 we use the LNA to analyse Google Flu Trends data from New Zealand, comparing the accuracy of week-ahead predictions with those from the recent approach of Dukic et al. (2012).

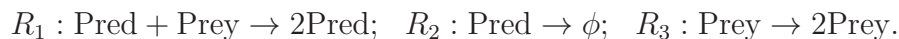
2. Reaction networks

Consider a general reaction of the form $B + C \rightarrow D$, where the number of elements of species B and C are respectively X_B and X_C and where the elements are distributed uniformly at random throughout some volume of space. The reaction occurs with some fixed probability whenever an element of species B is within some “reaction distance” of an element of C ; occurrences of the reaction may therefore be modelled as a Poisson process. With further, system dependent, assumptions, the rate, h , of the process is proportional to $X_B X_C$. Applying a similar argument, the rate of a reaction such as $B \rightarrow C$ is simply proportional to X_B and the rate of $2B \rightarrow C$ is proportional to $0.5X_B(X_B - 1)$. For a fuller discussion of mass-action kinetics see, for example, Gillespie (2005).

Consider now a network of n_r such reactions each involving at least one of the n_s species in the population. The dynamics of this model can be described by a vector of rates of the reactions together with a matrix which describes the effect of each reaction on the state. We denote by \mathbf{h} the n_r -vector of reaction rates. Now define A_{ij} be the net effect on species j of a single occurrence of reaction i : so $A_{ij} = 0$ means that the number of species j is unaffected by reaction i , whereas $A_{ij} = 1$ (or -1) means the number of species j will increase (or decrease) by 1. The $n_r \times n_s$ matrix \mathbf{A} is known as the net effect matrix. An equivalent way of defining the effect of a set of reactions is via the stoichiometry matrix, \mathbf{A}' , where throughout this article, $'$ denotes the transpose of a matrix.

Example 1: the Lotka-Volterra model

The Lotka-Volterra model (e.g. [Wilkinson, 2006](#)) describes a population of two competing species: *predators* which die with rate θ_2 and reproduce with rate θ_1 by consuming *prey* which reproduce with rate θ_3 . In its simplest form the probabilistic system is defined by:

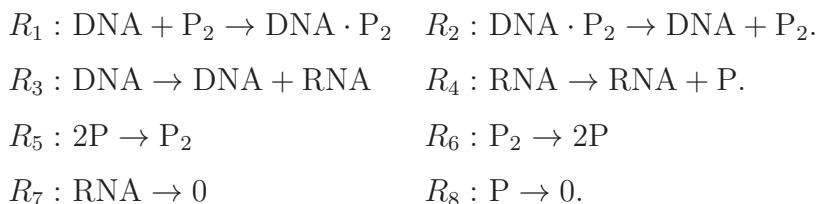


Denoting the number of Pred by X_1 and the number of Prey by X_2 gives the vector of reactions rates and the net effect matrix, respectively as:

$$\mathbf{h} := (\theta_1 X_1 X_2, \theta_2 X_1, \theta_3 X_2) \quad \text{and} \quad \mathbf{A}' = \begin{bmatrix} 1 & -1 & 0 \\ -1 & 0 & 1 \end{bmatrix}.$$

Example 2: autoregulatory gene network

The following system describes the self-regulating production of a protein, P, and its dimer, P₂. The system is analysed in [Golightly and Wilkinson \(2005\)](#) and is also discussed in [Wilkinson \(2006\)](#), while a similar system is analysed in [Golightly and Wilkinson \(2008\)](#). Reactions R_1 and R_2 describe the reversible process whereby the protein dimer P₂ binds to the gene (which we denote as DNA) and thereby inhibits the production, by reactions R_3 and R_4 , of the protein, P. Dimerisation of the protein and the reverse reaction are described by Reactions R_5 and R_6 , while R_7 and R_8 describe the destruction of the protein and of the enzyme RNA-polymerase, which is denoted RNA.



From the reactions, the total, k , of the number of DNA and DNA · P₂ molecules is fixed throughout the evolution of the system. Denoting the number of molecules of DNA, RNA, P, and P₂ as X_1 , X_2 , X_3 , and X_4 respectively therefore leads to a reaction rate vector of $\mathbf{h} := (\theta_1 X_1 X_4, \theta_2(k - X_1), \theta_3 X_1, \theta_4 X_2, \theta_5 X_3(X_3 - 1)/2, \theta_6 X_4, \theta_7 X_2, \theta_8 X_3)$. The net effect

matrix for this example is \mathbf{A} , where

$$\mathbf{A}' = \begin{bmatrix} -1 & 1 & 0 & 0 & 0 & 0 & 0 & 0 \\ 0 & 0 & 1 & 0 & 0 & 0 & -1 & 0 \\ 0 & 0 & 0 & 1 & -2 & 2 & 0 & -1 \\ -1 & 1 & 0 & 0 & 1 & -1 & 0 & 0 \end{bmatrix}.$$

Further examples, of a one and two-island epidemic model, are detailed in Appendix A.

3. Approximations for network evolution

We first consider the ODE and SDE approximations to the true process, and then sketch the justification for the Linear Noise Approximation (LNA).

It will be helpful to denote the n_s -vector holding the number of molecules of each species by \mathbf{X} and to define the $n_r \times n_r$ reaction rate matrix $\mathbf{H} := \text{diag}(\mathbf{h})$.

3.1 The ODE and SDE approximations

In an infinitesimal time dt the mean and variance of the change in \mathbf{X} due to all of the n_r independent Poisson processes can be calculated as (e.g. [Wilkinson, 2006](#)):

$$\mathbb{E}[d\mathbf{X}(t)] = \mathbf{A}'\mathbf{h} dt, \quad \text{Var}[d\mathbf{X}(t)] = \mathbf{A}'\mathbf{H}\mathbf{A} dt.$$

The ODE approximation to the evolution ignores the stochasticity of the model and is based solely on the expected change in the mean. This gives the following differential equation

$$\frac{d\mathbf{X}(t)}{dt} = \mathbf{A}'\mathbf{h}(\mathbf{X}(t), \boldsymbol{\theta}).$$

The SDE approximation models stochasticity through

$$d\mathbf{X}(t) = \mathbf{A}'\mathbf{h}(\mathbf{X}(t), \boldsymbol{\theta})dt + \sqrt{\mathbf{A}'\mathbf{H}(\mathbf{X}(t), \boldsymbol{\theta})\mathbf{A}} d\mathbf{W}(t),$$

where the matrix $\sqrt{\mathbf{A}'\mathbf{H}(\mathbf{X}(t), \mathbf{c})\mathbf{A}}$ is any (without loss of generality, $n_s \times n_s$) matrix square root, such as that obtained by Cholesky decomposition, and $\mathbf{W}(t)$ is Brownian motion.

The ODE model is deterministic, and fitting the model generally involves estimating both the initial condition and parameter values that give the best fit to the data. Often the fit

to the data is quantified by the sum of the square residuals (see [Ramsay et al., 2007](#), and references therein).

There are a range of methods for estimating parameters of an SDE model (see e.g. [Srensen, 2004](#)). Recently, there has been much research on how to implement likelihood-based methods (e.g. [Elerian et al., 2001](#); [Durham and Gallant, 2002](#); [Beskos et al., 2006](#); [Ait-Sahalia, 2008](#)). Generally, however, the SDE model will not lead to a tractable distribution for $\mathbf{X}(t)$ given \mathbf{X}_0 , and hence these models have an intractable likelihood. To overcome this complication it is common to approximate the transition density of the SDE, for example by the Euler approximation ([Kloeden and Platen, 1992](#)). The Euler approximation is only accurate over small time-intervals. The implementation of these methods therefore involves discretising time between each observation, and using computationally-intensive methods that impute values of the state at both the observation times and the grid of times between each observation. For example [Golightly and Wilkinson \(2005\)](#) implement such a method with an MCMC scheme, and [Golightly and Wilkinson \(2006\)](#) within a sequential Monte Carlo algorithm. There is a considerable computational overhead in implementing these methods which increases with the fineness of the grid of time-points between observations, and this has led to much research on efficient MCMC and other methods. See [Roberts and Stramer \(2001\)](#) for a discussion of how the fineness of the grid can affect mixing of the MCMC and, for example, [Golightly and Wilkinson \(2008\)](#) for details of more efficient MCMC approaches.

3.2 *The Linear Noise Approximation*

The Linear Noise Approximation (LNA) first appeared as a functional central limit law for density dependent processes; see [Kurtz \(1970\)](#) and [Kurtz \(1971\)](#) for the technical conditions. It approximates the dynamics of the network by an SDE which has tractable transition densities between observation times; inference therefore does not require any data augmentation ([van Kampen, 1997](#)).

Whilst Kurtz (1970) and Kurtz (1971) justify our use of the LNA it will be more helpful in the present context to consider the LNA as a general approximation to the solution to an SDE, and then apply this to the SDE model derived in the previous section. The idea of the LNA is that we partition $\mathbf{X}(t)$ into a deterministic path, $\boldsymbol{\eta}(t)$, and a stochastic perturbation from this path. Under the assumption that the perturbation is “small” relative to the deterministic path the distribution of an approximate solution at any given time point is found by solving a series of ODEs. In our applications the deterministic path is just the solution of the ODE model introduced in the previous section. Here we provide a short heuristic motivation of the approximation; for a more rigorous derivation and more detailed discussion the reader is referred to Ferm et al. (2008).

Consider the general SDE for vector \mathbf{X} of length n_s

$$d\mathbf{X}(t) = \mathbf{a}(\mathbf{X}(t)) dt + \epsilon \mathbf{S}(\mathbf{X}(t)) d\mathbf{W}(t), \quad (1)$$

with initial condition $\mathbf{X}(0) = \mathbf{X}_0$. Let $\boldsymbol{\eta}(t)$ be the (deterministic) solution to

$$\frac{d\boldsymbol{\eta}}{dt} = \mathbf{a}(\boldsymbol{\eta}) \quad (2)$$

with initial value $\boldsymbol{\eta}_0$. We assume that over the time interval of interest $\|\mathbf{X} - \boldsymbol{\eta}\|$ is $O(\epsilon)$. Set $\mathbf{M}(t) = (\mathbf{X}(t) - \boldsymbol{\eta}(t))/\epsilon$ and use a Taylor expansion of \mathbf{a} and \mathbf{S} about $\boldsymbol{\eta}(t)$ in (1). Collecting terms of $O(\epsilon)$ gives

$$d\mathbf{M}(t) = \mathbf{F}(t)\mathbf{M}(t) dt + \mathbf{S}(t) d\mathbf{W}(t), \quad (3)$$

where \mathbf{F} is the $n_s \times n_s$ matrix with components

$$F_{ij}(t) = \left. \frac{\partial a_i}{\partial x_j} \right|_{\boldsymbol{\eta}(t)}, \quad \text{and} \quad \mathbf{S}(t) = \mathbf{S}(\boldsymbol{\eta}(t)).$$

The use of ϵ in (1) is purely to indicate that the stochastic term $\epsilon \mathbf{S}(\mathbf{X}(t))$ is “small” relative to the drift, and to aid in the collection of terms of similar size. Henceforth it will be simpler to set $\epsilon = 1$ and assume that $\mathbf{S}(\mathbf{X}(t))$ is “small”. The initial condition for (3) is therefore $\mathbf{M}_0 = (\mathbf{X}_0 - \boldsymbol{\eta}_0)$.

Provided that \mathbf{X}_0 has either a point mass at \mathbf{x}_0 or has a Gaussian distribution, the increment in (3) is a linear combination of Gaussians so $\mathbf{M}(t)$ has a Gaussian distribution for all t . The mean and variance of this Gaussian can be obtained by solving a series of ODEs,

$$\frac{d\mathbf{m}}{dt} = \mathbf{F}\mathbf{m}, \quad (4)$$

$$\frac{d\mathbf{\Psi}}{dt} = \mathbf{\Psi}\mathbf{F}^t + \mathbf{F}\mathbf{\Psi} + \mathbf{S}\mathbf{S}^t, \quad (5)$$

where $\mathbf{m}(t) := \mathbb{E}[\mathbf{M}(t)]$, and $\mathbf{\Psi}(t) := \text{Var}[\mathbf{M}(t)]$ (see Appendix B for the derivation).

Suppose $\mathbf{X}_0 \sim N(\boldsymbol{\mu}_0^*, \boldsymbol{\Sigma}_0^*)$, then for arbitrary $\boldsymbol{\eta}_0$ we may set $\boldsymbol{\eta}(0) = \boldsymbol{\eta}_0$, $\mathbf{m}(0) = \boldsymbol{\mu}_0^* - \boldsymbol{\eta}_0$ and $\mathbf{\Psi}(0) = \boldsymbol{\Sigma}_0^*$. Integrating (2), (4) and (5) through to time t provides the LNA approximation

$$\mathbf{X}_t \sim N(\boldsymbol{\eta}(t) + \mathbf{m}(t), \mathbf{\Psi}(t)). \quad (6)$$

Transition probabilities for the autoregulatory model (Example 2) given by the LNA and estimated from the SDE approximation were compared with estimates of the true probabilities for three different system sizes (see Appendix C for details). The results suggest that even for relatively small system sizes LNA transition probabilities are comparable with those from the SDE and can provide a reasonable approximation to the probabilities under the MJP.

4. Inference using the LNA

We first briefly describe the inference methodology when we observe a system exactly and completely at a discrete set of times. We then show how to perform inference when only linear combinations of a subset of species are observed, and these, potentially, are observed with error. Finally we compare our approach with an alternative method of using the LNA for inference introduced by [Komorowski et al. \(2009\)](#).

4.1 The fully and exactly observed system

Consider the situation where at each of a discrete set of times, t_i ($i = 0, \dots, n$), the system, \mathbf{x}_i , is observed completely and without error. Let the true transition density of the system be denoted by $\pi(\mathbf{x}_i|\mathbf{x}_{i-1}, \theta)$ and the LNA approximation of this by $\hat{\pi}_{LNA}(\mathbf{x}_i|\mathbf{x}_{i-1}, \theta)$. In practice we use the LNA approximation obtained using $\boldsymbol{\eta} = \mathbf{x}_i$, $\mathbf{m} = \mathbf{0}$, $\boldsymbol{\Psi} = \mathbf{0}$. This implementation is based on an ODE solution that is piecewise continuous, with discontinuities at observation times as we restart each ODE solution at the observations. Further, as $\mathbf{m}(t_i) = \mathbf{0}$, directly from (4) we have $\mathbf{m}(t) = \mathbf{0}$ for all $t > t_i$.

For a fully observed system, the likelihood factorises as $L(\theta) = \prod_{i=1}^n \pi(\mathbf{x}_i|\mathbf{x}_{i-1}, \theta)$. This motivates using the approximation: $\hat{L}_{LNA}(\theta) = \prod_{i=1}^n \hat{\pi}_{LNA}(\mathbf{x}_i|\mathbf{x}_{i-1}, \theta)$. The approximation is a product of Normal densities, with the mean and covariances depending on the parameters. It is possible to maximise this likelihood numerically. Alternatively, if we introduce priors for θ , $\pi(\theta)$, we can use standard MCMC algorithms to sample from the corresponding approximation to the posterior which is proportional to $\pi(\theta)\hat{L}_{LNA}(\theta)$.

The accuracy of estimators obtained by maximising $\hat{L}_{LNA}(\theta)$ has been extensively studied in Giagos (2011), for both the Lokta-Volterra model (Example 1), and the auto-regulatory model (Example 2). The method gave reliable point estimates of parameters, and reasonable estimates of uncertainty (coverage of 95% confidence intervals was generally 90% for small systems, and close to 95% for large systems).

4.2 Partially-observed systems

Now assume that we have partial observations $\mathbf{y}_0, \dots, \mathbf{y}_n$ from times $0 = t_0, \dots, t_n = T$, where the conditional distribution for the observations given the true process is

$$\mathbf{Y}_i|\mathbf{x}_i \sim N(\mathbf{P}(\boldsymbol{\theta})\mathbf{x}_i, \mathbf{V}(\boldsymbol{\theta})).$$

For the examples in Section 5 the matrix $\mathbf{P}(\boldsymbol{\theta})$ simply removes certain components of \mathbf{x}_i and leaves the remaining components unchanged; an operation that requires no parameterisation,

but for the model analysed in Section 6 the observations are centered on an unknown but fixed multiple of the true values (with Gaussian error). The variance of the Gaussian error, \mathbf{V} , can be any deterministic function (of time, for example) parameterised by $\boldsymbol{\theta}$. In the examples that we consider in this article \mathbf{V} is either $\mathbf{0}$ or a fixed (unknown) diagonal matrix. We also introduce a prior, $\mathbf{X}_0 \sim N(\boldsymbol{\mu}_0, \boldsymbol{\Sigma}_0)$. To simplify notation, in the following we drop the explicit dependence of the matrices $\mathbf{P}(\boldsymbol{\theta})$ and $\mathbf{V}(\boldsymbol{\theta})$ on $\boldsymbol{\theta}$. We will also use $\mathbf{y}_{0:i} := (\mathbf{y}_0, \dots, \mathbf{y}_i)$.

4.2.1 *Approximating the Likelihood using the LNA.* Any likelihood may be decomposed as

$$L(\boldsymbol{\theta}) = \pi(\mathbf{y}_0|\boldsymbol{\theta}) \prod_{i=1}^n \pi(\mathbf{y}_i|\mathbf{y}_{0:i-1}, \boldsymbol{\theta}).$$

Firstly, $\pi(\mathbf{y}_0)$ can be calculated directly from our model as $\mathbf{Y}_0 \sim N(\mathbf{P}\boldsymbol{\mu}_0, \mathbf{P}\boldsymbol{\Sigma}_0\mathbf{P}^t + \mathbf{V})$. We then calculate approximations $\hat{\pi}_{LNA}(\mathbf{y}_i|\mathbf{y}_{0:i-1}, \boldsymbol{\theta})$ to $\pi(\mathbf{y}_i|\mathbf{y}_{0:i-1}, \boldsymbol{\theta})$ recursively for $i = 1, \dots, n$.

Standard results give $\mathbf{X}_0|\mathbf{y}_0 \sim N(\boldsymbol{\mu}_0^*, \boldsymbol{\Sigma}_0^*)$, where

$$\begin{aligned} \boldsymbol{\mu}_0^* &= \boldsymbol{\mu}_0 + \boldsymbol{\Sigma}_0\mathbf{P}^t (\mathbf{P}\boldsymbol{\Sigma}_0\mathbf{P}^t + \mathbf{V})^{-1} (\mathbf{y}_0 - \mathbf{P}\boldsymbol{\mu}_0) \\ \boldsymbol{\Sigma}_0^* &= \boldsymbol{\Sigma}_0 - \boldsymbol{\Sigma}_0\mathbf{P}^t (\mathbf{P}\boldsymbol{\Sigma}_0\mathbf{P}^t + \mathbf{V})^{-1} \mathbf{P}\boldsymbol{\Sigma}_0. \end{aligned}$$

We then apply Kalman filter recursions and the LNA, repeating the following steps:

- (1) **Obtain the predictive distribution at time t_i .**

We will have that for suitable $\boldsymbol{\mu}_{i-1}^*$ and $\boldsymbol{\Sigma}_{i-1}^*$:

$$\mathbf{X}_{i-1}|\mathbf{y}_{0:i-1} \sim N(\boldsymbol{\mu}_{i-1}^*, \boldsymbol{\Sigma}_{i-1}^*).$$

We then initiate the LNA with $\boldsymbol{\eta}(t_{i-1}) = \boldsymbol{\mu}_{i-1}^*$, so that $\mathbf{m}(t_{i-1}) = \mathbf{0}$, and $\boldsymbol{\Psi}(t_{i-1}) = \boldsymbol{\Sigma}_{i-1}^*$.

From (4), $\mathbf{m}(t_i) = \mathbf{0} \Rightarrow \mathbf{m}(t) = \mathbf{0}$ for all $t > t_i$. Further, integrating the ODEs (2) and (5) forward for time $t_i - t_{i-1}$ provides $\boldsymbol{\eta}(t_i)$ and $\boldsymbol{\Psi}(t_i)$, so that our approximation to the density at t_i is $\mathbf{X}_i|\mathbf{y}_{1:i-1} \sim N(\boldsymbol{\mu}_i, \boldsymbol{\Sigma}_i)$, where $\boldsymbol{\mu}_i = \boldsymbol{\eta}(t_i)$ and $\boldsymbol{\Sigma}_i = \boldsymbol{\Psi}(t_i)$.

- (2) **Calculate $\hat{\pi}_{LNA}(\mathbf{y}_i|\mathbf{y}_{0:(i-1)}, \boldsymbol{\theta})$.**

Using $\mathbf{Y}_i = \mathbf{P}\mathbf{X}_i + \epsilon_i$, where $\epsilon_i \sim N(0, \mathbf{V})$ directly gives

$$\mathbf{Y}_i | \mathbf{y}_{0:i-1} \sim N(\mathbf{P}\boldsymbol{\mu}_i, \mathbf{P}\boldsymbol{\Sigma}_i\mathbf{P}^t + \mathbf{V}).$$

(3) **Calculate** $\hat{\pi}_{LNA}(\mathbf{x}_i | \mathbf{y}_{0:i}, \theta)$.

Since

$$\begin{bmatrix} \mathbf{X}_i \\ \mathbf{Y}_i \end{bmatrix} | \mathbf{y}_{1:(i-1)} \sim N \left(\begin{bmatrix} \boldsymbol{\mu}_i \\ \mathbf{P}\boldsymbol{\mu}_i \end{bmatrix}, \begin{bmatrix} \boldsymbol{\Sigma}_i & \boldsymbol{\Sigma}_i\mathbf{P}^t \\ \mathbf{P}\boldsymbol{\Sigma}_i & \mathbf{P}\boldsymbol{\Sigma}_i\mathbf{P}^t + \mathbf{V} \end{bmatrix} \right) \quad (7)$$

we have directly that $\mathbf{X}_i | \mathbf{y}_{1:i} \sim N(\boldsymbol{\mu}_i^*, \boldsymbol{\Sigma}_i^*)$, where

$$\boldsymbol{\mu}_i^* = \boldsymbol{\mu}_i + \boldsymbol{\Sigma}_i\mathbf{P}^t (\mathbf{P}\boldsymbol{\Sigma}_i\mathbf{P}^t + \mathbf{V})^{-1} (\mathbf{y}_i - \mathbf{P}\boldsymbol{\mu}_i) \quad (8)$$

$$\boldsymbol{\Sigma}_i^* = \boldsymbol{\Sigma}_i - \boldsymbol{\Sigma}_i\mathbf{P}^t (\mathbf{P}\boldsymbol{\Sigma}_i\mathbf{P}^t + \mathbf{V})^{-1} \mathbf{P}\boldsymbol{\Sigma}_i. \quad (9)$$

Our approximation for the likelihood of the data is then

$$\hat{L}_{LNA}(\boldsymbol{\theta}) = \pi(\mathbf{y}_0 | \theta) \prod_{i=1}^n \hat{\pi}_{LNA}(\mathbf{y}_i | \mathbf{y}_{0:i-1}, \theta). \quad (10)$$

The only approximation in $\hat{L}_{LNA}(\boldsymbol{\theta})$ is due to using the LNA for the transition density of the system, which gives us the Normal approximation to $\mathbf{X}_i | \mathbf{y}_{1:i-1}$ from the Normal approximation to $\mathbf{X}_{i-1} | \mathbf{y}_{1:i-1}$.

We emphasise that in Step (1), once the observation \mathbf{y}_{i-1} is available then for the period of integration from t_{i-1} to t_i we *re-initialise* the ODE (2) to the posterior mean at t_{i-1} by setting $\eta(t_{i-1}) = \boldsymbol{\mu}_{i-1}^*$, leading to a piecewise-continuous solution for η . The LNA relies on a first-order Taylor expansion about η , and by continually realigning the point about which the expansion is performed to the current best estimate of the centre of the distribution we aim to minimise the impact of the higher-order terms that have been neglected.

4.3 MCMC scheme

It is possible to estimate the parameters by numerically maximising the LNA approximation to the likelihood (10). However we consider a Bayesian analysis. We introduce priors for the parameters, $\pi(\boldsymbol{\theta})$, and use MCMC to generate samples from the resulting approximation to the posterior $\pi(\boldsymbol{\theta}) \hat{L}_{LNA}(\boldsymbol{\theta})$.

We implemented a random-walk Metropolis algorithm (RWM). Each iteration of the algorithm involved a single block update of all the log-parameters. Using the log-scale is natural as all parameters are positive. For the simulation study in Section 5 we used pilot runs to tune our algorithms (and algorithms against which we compare): the covariance of the random-walk proposal was proportional to the estimate of the covariance of the posterior from the pilot run, with the scale tuned to produce an acceptance rate in the range 0.25–0.30 (Roberts and Rosenthal, 2001). For the analysis of the Google Flu Trends Data in Section 6 we used an adaptive RWM algorithm similar to that in Sherlock et al. (2010).

4.4 Implementation

The ODEs required for calculating $\pi(\mathbf{y}_i | \mathbf{y}_{0:(i-1)})$ can be solved numerically. Care is needed as in many applications the ODEs are stiff (Hairer and Wanner, 1991). There are standard numerical routines for solving stiff ODEs, and we used the `lsoda` package (Petzold, 1983).

4.5 Alternative use of the LNA

Previously, use of the LNA for Bayesian inference on stochastic kinetic networks has been suggested by Komorowski et al. (2009), but their implementation has important differences from ours. The approach of Komorowski et al. (2009) involves using the LNA to obtain an approximation for the joint distribution of $\mathbf{X}_{1:n} = (\mathbf{X}_1, \dots, \mathbf{X}_n)$ conditional on a value for \mathbf{x}_0 . This can be combined with the linear-Gaussian relationship between each observation \mathbf{Y}_i and state-value \mathbf{X}_i to give an approximation to the likelihood for data $\mathbf{y}_{1:n}$ in terms of the parameters, $\boldsymbol{\theta}$ and the initial value, \mathbf{x}_0 . They introduce priors for the $\boldsymbol{\theta}$ and \mathbf{x}_0 , and sample from the (approximate) posterior for these using MCMC.

In practice the most important difference between this approach and ours, is that Komorowski et al. (2009) use the LNA over a time period $[0, t_n]$ obtained from solving the ODE approximation to the model over this period for a given initial condition. By comparison we use a different LNA for each time-interval $[t_{i-1}, t_i]$, essentially restarting the LNA using the posterior mean

of \mathbf{x}_{t-1} given $\mathbf{y}_{0:t-1}$ as the initial condition for the ODE (2). This difference can be important for some models, as the ODE solution can become poor over long time-periods. Thus the approach of Komorowski et al. (2009) can give a poor approximation to the distribution of \mathbf{X}_t for larger values of t . By re-starting the LNA method over each time-interval we help avoid the problems of the approximation getting worse for larger t .

The difference in accuracy of the two approaches for using the LNA is investigated thoroughly for systems which are fully observed at discrete time-points in Giagos (2011), where the method of Komorowski et al. (2009) was found to be less accurate, for both point and interval estimation, than the method we introduce above. We further demonstrate the increased accuracy of our approach for partially-observed systems in Section 5.

5. Simulation study

We now empirically evaluate the performance of the LNA for inference on parameters in both the Lotka-Volterra model (Example 1) and the auto-regulatory model (Example 2). Our aim is to both compare our approach with inference based on ODE approximations, the LNA approach of Komorowski et al. (2009), and the SDE-based approach of Golightly and Wilkinson (2005); and to evaluate the accuracy obtained by using the LNA for both point and interval estimation.

The code of Golightly and Wilkinson (2005) was adapted to use the same half-Cauchy prior for the parameters as us and to employ an optimally-tuned single-block RWM Gaussian proposal so that this aspect would be exactly comparable with our RWM scheme. All MCMC algorithms except for that of Golightly and Wilkinson (2005) were run for 110,000 iterations, from which the first 5,000 iterations were discarded as burn-in. Output from simulations for the autoregulatory system was thinned by a factor of 10 for storage. Since it mixed more slowly the algorithm of Golightly and Wilkinson (2005) was run for 260,000 iterations with

a burn-in of 10,000 iterations; as with the LNA-based analysis of the autoregulatory system, output was thinned by a factor of 10.

In assessing accuracy of a method on a given model, throughout we present results based on analysing 100 different data sets simulated using the true jump process for a given model and set of parameter values. We present results in terms of estimating the log of the parameter since interest is primarily in the order of magnitude of the reaction rates. The posterior median is used as the point estimate for each parameter as this is both invariant to monotonic transformations and is robust to heavy-tailed posterior distributions.

5.1 Comparison with ODE method and Komorowski et al.

Our first comparison is with approximating the evolution as a deterministic ODE, and with the LNA method of Komorowski et al. and is based on the Lotka-Volterra model. We simulated data with $\mathbf{X}_0 = (40, 140)$ and with $\theta_1 = 0.01$, $\theta_2 = 0.6$ and $\theta_3 = 0.3$. Observations were made every second for 30 seconds, or until one of the species became extinct. We used Gamma(2,10) priors for all rate parameters, which gave a reasonable prior mass across the range of values the rates take. We assumed that predators are observed exactly for the LNA method and for that of Komorowski et al., and the prey are unobserved.

The ODE method uses a log-likelihood (and hence log-posterior) which depends on the sum of squared errors between the solution of the ODE and the observations, and is equivalent to modelling the observations as having additive Gaussian error; we place a half-Cauchy prior on the error variance, $\pi(\sigma^2) \propto 1/(1 + \sigma^4)$. Both LNA methods have a similar computational cost, while the ODE approach has a smaller computational cost as the differential equations for the variance in the LNA need not be solved.

[Table 1 about here.]

Results are shown in Table 1. The new LNA approach is uniformly better at estimating each parameter in terms of both accuracy of point estimates and coverage of credible intervals. The

approach of Komorowski et al. is in turn more accurate than using an ODE approximation. These results are for a small system, and the difference between the different approaches will be less if a larger system size is studied.

To see why the new LNA approach is more accurate than either that of Komorowski et al. or that of using an ODE approximation, it is useful to see results from a single dataset. In Figure 1 we show a simulated data set, together with the best fitting ODE solution. This solution gives a poor fit to the data, and as the LNA of Komorowski is based on such ODE solutions, that approach gives a poor approximation to the likelihood. By comparison, as our approach re-starts the LNA at each observation, we get a good approximation to the likelihood terms across the whole time-period of the data.

[Figure 1 about here.]

5.2 Comparison with SDE approach of Golightly and Wilkinson

We now compare our method with an approach based on an SDE approximation to the model (Golightly and Wilkinson, 2005). We compare on the auto-regulatory model (Example 2) with observations every half a second for 25 seconds with the parameter values detailed in Table 2. We considered models where all components of the system are observed without error, as the code that implements the approach of (Golightly and Wilkinson, 2005) assumes this observation model. For both inference methods we assumed independent half-cauchy priors, $\pi(\theta_i) \propto 1/(1 + (2\theta_i)^2)$ for $\theta_i > 0$ for all i .

The method of Golightly and Wilkinson (2005) involves imputing the path of the SDE at $m - 1$ time-points in between each observation. We present results for $m = 10$, which gave a good trade-off between accuracy and computational efficiency.

As well as comparing the accuracy of point and interval estimates for the two methods, we also compare the computational efficiency. To do this we calculated the integrated auto-

correlation time for each parameter, and from this the Effective Sample Size (ESS). We summarise results in terms of the ESS divided by CPU time.

[Table 2 about here.]

Results are given in Table 2. The comparative performance of the two methods varies with parameter. For the parameters θ_3 , θ_4 , θ_7 and θ_8 , both methods are similar in terms of accuracy and of size and coverage of credible intervals. Coverage of credible intervals are consistent with their nominal size. Computational efficiency of the two methods is also very similar, with a mean ESS per second of 0.84 and 0.80 for the LNA and SDE methods respectively.

However inference on the remaining parameters differs considerably. The SDE method is uniformly more accurate, and has substantially smaller credible intervals in all cases. For both methods, coverage of credible intervals is close to 90% for these parameters. The computational efficiency of the LNA is substantially higher for these parameters with the ESS per second an order of magnitude greater.

The parameters for which the inferences of the two methods differ consist of two pairs of reaction rates: θ_1 and θ_2 are the rates of reversible reactions linked to the product $\text{DNA} \cdot \text{P}_2$, whereas θ_5 and θ_6 are the rates of reversible reactions linked to the dimerisation of the protein. As such we would expect difficulty in estimating each rate individually, as increasing both θ_1 and θ_2 , say, together would lead to similar data. The larger credible intervals produced by the LNA are consistent with this. Investigating the performance of the SDE approximation shows that the Euler discretisation becomes increasingly inaccurate as the parameter vector increases. Changes in the state vector over a discretisation interval Δt from a system with rate parameters $k\boldsymbol{\theta}$ have exactly the same distribution as changes in the state vector over an interval $k\Delta t$ with rate parameters $\boldsymbol{\theta}$. For $k > 1$ this decreases the accuracy of the estimated likelihood. In general therefore the Euler method will not estimate the posterior well for large rates.

To investigate this further we considered a second example, with all rate parameters increased by a factor of 4. This gives insight into whether the method of Golightly and Wilkinson (2005) is producing appropriate credible intervals for these parameters, or whether the method is biased towards smaller parameter values, which happened to be consistent with the true parameter values used for the first simulation study.

Detailed results are given in Table 1 of Appendix D. We observe poor inference for θ_1 , θ_2 , θ_5 and θ_6 using the method of Golightly and Wilkinson (2005): accuracy is lower than using the LNA, and the credible intervals are too small, leading to coverage probabilities less than 0.5 in all cases. However, the method of Golightly and Wilkinson (2005) does give more accurate inferences for the remaining parameters. This is likely to be because the extra variability arising from the larger rates means that the perturbations of the system from the ODE solution are no longer small.

5.3 Accuracy of the LNA method

We further investigate the accuracy of the LNA, by repeating the analysis of the auto-regulatory example, but considering different observation models. We considered all components observed with error, and only three components observed either exactly or with Gaussian error; errors for each species were independent with mean zero and variance 1. We use the same priors as above.

Results are given in Appendix D and are comparable with those in Table 2. The LNA appears to provide good estimates of the parameters. As we would expect, as we observed fewer species, or observe with error, the uncertainty in our estimates increases. Perhaps most importantly, the coverage rates we obtain are close to 95% in all cases, suggesting the method is giving a good estimate of uncertainty. We obtain higher coverage rates with less informative data, possibly because any bias in the LNA has less effect when we have higher posterior variance.

6. Prediction of Flu Epidemics using Google Flu Trends Data

We now apply our method to predict flu case numbers based on data from Google Flu Trends (GFT; <http://www.google.org/flutrends>). GFT data are estimates of the number of new cases of flu each week (per 100,000 people) based on the popularity of terms associated with flu in web searches. [Ginsberg et al. \(2009\)](#) showed that actual numbers of flu cases can be accurately predicted using such data, with the advantage of being able to obtain estimates of the current number of cases, as opposed to health-service data which are typically published with a delay of approximately one week and are often incomplete.

Our analysis is motivated by [Dukic et al. \(2012\)](#), who use a one-compartment SEIR model (see Appendix A for details) to show that accurate predictions of flu cases can be obtained from GFT data using a state-space SEIR model, and in particular that such models are substantially more accurate than simple AR models. For our analysis we consider cases in the North and South Islands of New Zealand. GFT data were obtained for each island, for January 2008 to January 2012 inclusive, and converted from proportions into counts.

Each year there is a flu epidemic, often with different flu strains. The number of flu cases in New Zealand is typically at its yearly minimum around the start of February, and so we split our data into four separate ‘years’ from February yr to January of $yr + 1$ for $yr \in \{2008, 2009, 2010, 2011\}$.

We model the data using a two-compartment SEIR model. Our state consists of the number of susceptibles, exposed, infected and recovered in each of the north and south islands. We assume a fixed population size for both islands, which results in a 6-dimensional state: $\{S_1, E_1, I_1, S_2, E_2, I_2\}$, where a subscript of 1 denotes North Island and a subscript of 2 denotes South Island.

The reactions in our model are:

$$\begin{aligned}
R_1 : S_1 + I_1 &\rightarrow E_1 + I_1 & R_2 : S_2 + I_2 &\rightarrow E_2 + I_2 \\
R_3 : E_1 &\rightarrow I_1 & R_4 : E_2 &\rightarrow I_2 \\
R_5 : I_1 &\rightarrow 0 & R_6 : I_2 &\rightarrow 0 \\
R_7 : S_1 + I_2 &\rightarrow E_1 + I_2 & R_8 : S_2 + I_1 &\rightarrow E_2 + I_1
\end{aligned}$$

Further details of the model are provided in Appendix A.

Observations are $\mathbf{y}_t = (y_t^{(1)}, y_t^{(2)})$, the number of flu cases, from the GFT data, in week t in the North and South Island respectively. We model that these are realisations of random variables $Y_t^{(j)}$, for $j = 1, 2$, where $Y_t^{(j)} \sim \text{N}(CI_j(t), \sigma_j^2)$. A heuristic interpretation is that our SEIR models apply to the number of ‘communities’ that are infected, and assume an equal rate of contact between each pair of communities. If a community is infected, then C is the average number of flu cases that will result. Priors follow a similar form to those in [Dukic et al. \(2012\)](#); full details are given in Appendix E.

For each year’s data, and for each $t = 2, \dots, 51$ we use Steps (1)-(3) in Section 4.2.1 within an adaptive RWM algorithm similar to that in [Sherlock et al. \(2010\)](#) (see Appendix F) to estimate both the parameters and the current state of the model given observations $\mathbf{y}_{1:t}$. For each sample from the RWM we then apply Step (1) again to predict the number of cases in week $t + 1$.

As a benchmark to compare with, we also analysed the data using the method of [Dukic et al. \(2012\)](#). This approach uses sequential Monte Carlo (SMC), and we shall refer to it as the SMC approach. It is based on fitting a single compartment SEIR model (henceforth 1CM) to data on the total number of flu cases across both islands. To deal with the intractability of the Markov jump model, the ODE approximation (2) is used and is itself approximated using an Euler scheme with a discretisation of the inter-observation interval (here one week). Gaussian noise is then added to the relative change in the number of infectives between observation times, leading to a very different Gaussian transition model to (6). The observation model is also based on the relative change in the number of infectives, with additive errors assumed

to be Gaussian. The SMC scheme approximates the joint posterior for the parameters and the state at time t , given the data up to time t , by a set of weighted particles. Due to the choice of approximations of both the state dynamics and the observation, efficient methods (Carvalho et al., 2010; Pitt and Shephard, 1999) for implementing the SMC algorithm can be used. See Dukic et al. (2012) for more details.

One advantage of this approach is computational, as, unlike with MCMC, the algorithm does not need to be re-run from scratch each time a new observation is received. The potential disadvantage of the method is that it uses a cruder approximation to the underlying jump-Markov model.

We attempted to implement an equivalent SMC approach to fit a two component SEIR model (henceforth 2CM) to the Google flu-trends data. However results from the SMC analysis of this model, using 10^7 particles, were substantially worse than for the 1CM. SMC methods are known to often perform poorly for models with unknown parameters. The poor results for the 2CM are thus likely to be due to poor Monte Carlo performance for a model with 10 unknown parameters. For further comparability with the method of Dukic et al. (2012) we therefore also analysed data for the whole of New Zealand using the LNA within a 1CM.

For each LNA analysis we ran an MCMC for 100,000 iterations, using a burn-in of 20,000 for the 2CM and of 10,000 for the 1CM (then thinning both by a factor of 10). For a week-ahead prediction at the height of the flu season (after 30 weeks of data) runs for the 1CM model took between 150 and 156 seconds on a single Intel Core i7 3770 CPU@3.40GHz, while runs for the 2CM took between 1054 and 1135 seconds. Repeated runs of the MCMC produced the same estimates of accuracy to at least two significant figures. The SMC analysis achieved a similar precision to the LNA when 10^6 particles were used. Week-ahead predictions from 30 weeks of data took between 67.7 and 68.1 seconds.

[Table 3 about here.]

Summaries of the accuracy of both models using the LNA and of the 1CM using SMC in predicting the total number of cases across both islands, and the coverage of 95% credible intervals for the predictions are given in Table 3. Compared to the SMC method we see that, for all four years, the LNA (using either model) gives less biased estimates and smaller forecast error, as measured by the mean absolute error in predictions. The credible intervals produced by the LNA methods are at least a factor of 5 smaller than for the approach of [Dukic et al. \(2012\)](#). However the coverage of the LNA's credible intervals is between 80% and 86%. We believe the reason for this is most likely due to our model assuming a constant variance for the observation error, whereas the variance of this error appears to increase with the current size of the epidemic. We thus under-estimate the uncertainty at the peak of the flu epidemic. From the table, predictions for New Zealand as a whole from the 2CM are no better than those from the 1CM, however the 2CM also provides individual predictions for North and South Island. These predictions, together with the true number of cases (as given by the Google Flu Trends data), are shown in Figure 2 in Appendix D; summaries of the accuracy are provided in Table 3 of the same appendix.

7. Discussion

We have demonstrated how the LNA can be used to perform inference for reaction networks where all, or a subset, of components are observed. Observations can either be exact, or with additive Gaussian error. Results suggest that using the LNA is more accurate than approximating the underlying model using an ODE.

The LNA is based upon first obtaining a deterministic approximation to the path of the state vector over time; and then modelling the error about this deterministic approximation. Key to the error in the LNA being small is that the deterministic approximation is

accurate. We have shown that recalculating the deterministic solution between each pair of observations is more accurate than calculating a single deterministic solution as suggested by [Komorowski et al. \(2009\)](#). Furthermore, across the examples we looked at the LNA gives reliable inferences in almost all cases. The one exception (for a subset of parameters in the results in Table 1 of Appendix C) corresponds to cases where the noise in the model was high, leading to the perturbations of the system about the deterministic solution not being small.

We have also compared with a method based on approximating the underlying model using an SDE. The accuracy of the LNA and SDE-based approaches are similar, with the relative performance of the two approaches varying depending on which reaction rates are being estimated. The advantage of the LNA is one of simplicity – as the LNA gives an analytic form for the approximation to the transition density of the model. In particular there is no need to choose a level of time-discretisation. Calculating the LNA involves solving a set of ODEs, but standard routines exist for appropriately choosing and adapting the step-size using in numerically solving the ODEs. By comparison SDE methods currently involve the user pre-specifying the level of time-discretisation. Choosing an appropriate level is difficult, partly because the required level needed to get an accurate approximation can depend on the parameter values, and these will change at each MCMC iteration.

We have demonstrated the usefulness of the LNA for inference by making predictions for flu cases in New Zealand using Google Flu Trends data. Whilst our prediction accuracy was higher than that of [Dukic et al. \(2012\)](#), our assumption of a constant observation variance leads to us under-estimating uncertainty in future observations at the peak of the epidemic. This assumption is currently needed for the tractability of our algorithm, but it should be possible to relax this assumption, for example using ideas from [Rue et al. \(2009\)](#) to allow for efficient inference under a range of observation models.

We considered fitting a two-compartment SEIR model to the New Zealand data, but the scalability of the LNA should mean it is possible to analyse SEIR models with even more compartments – for example to jointly analyse data from multiple cities in the US. For a reaction network with n_r reactions and a state-space of size n_s , the LNA requires the numerical integration of n_s^2 ODEs, with $O(n_r)$ rate-related calculations at each time-point. For the two-compartment model, the state-space was twice the size of that of the one-compartment model, and the number of reactions more than doubled. Given the other computational overheads of the algorithm, this is consistent with the observed increase in CPU time by a factor of approximately 7, and, given the short running time for the two-compartment model (less than 20 minutes), suggests that on-line week-ahead predictions should be feasible for models with three or four compartments.

The approach of [Dukic et al. \(2012\)](#) uses a sequential Monte Carlo algorithm, which is computationally more convenient than MCMC. SMC inference for the single-compartment model of [Dukic et al. \(2012\)](#) was more than twice as fast as the single compartment LNA, but we could not implement an accurate SMC method for the two-component model. This seems to be due to problems with using SMC to analyse models with moderately large numbers of parameters. Alternative sequential Monte Carlo approaches, such as those based on mode tracking (e.g. [Vaswani, 2008](#)), have recently been shown to be accurate for high-dimensional state processes, and may offer a competitive alternative for analysing data such as that from Google Flu Trends.

8. Supplementary Materials

Web Appendices A, B, C, D, E and F, referenced respectively in Sections [2](#), [3.2](#), [3.2](#), [5.2](#), [6](#) and [6](#), are available with this paper at the Biometrics website on Wiley Online Library. The supplementary material also contains C code implementing the LNA for all of the models considered in this article.

ACKNOWLEDGEMENTS

The authors are grateful to Dr. A. Golightly for supplying C code for inference on the completely and exactly observed autoregulatory example using the methodology in [Golightly and Wilkinson \(2005\)](#), and to Dr. V. Dukic for supplying the R code for prediction from the Google Flu Trends data using the methodology in [Dukic et al. \(2012\)](#). Paul Fearnhead was supported by EPSRC grant EP/G028745.

REFERENCES

- Ait-Sahalia, Y. (2008). Closed-form likelihood expansions for multivariate diffusions. *Annals of Statistics* **36**, 906–937.
- Amrein, M. and Künsch, H. (2012). Rate estimation in partially observed markov jump processes with measurement errors. *Statistics and Computing* **22**, 513–526. 10.1007/s11222-011-9244-1.
- Andersson, H. and Britton, T. (2000). *Stochastic epidemic models and their statistical analysis*, volume 151 of *Lecture Notes in Statistics*. Springer-Verlag, New York.
- Ball, F. and Neal, P. (2008). Network epidemic models with two levels of mixing. *Math. Biosci.* **212**, 69–87.
- Beskos, A., Papaspiliopoulos, O., Roberts, G. O., and Fearnhead, P. (2006). Exact and computationally efficient likelihood-based estimation for discretely observed diffusion processes (with discussion). *Journal of the Royal Statistical Society Series B* **68**, 333–382.
- Boys, R. J., Wilkinson, D. J., and Kirkwood, T. B. L. (2008). Bayesian inference for a discretely observed stochastic kinetic model. *Stat. Comput.* **18**, 125–135.
- Carvalho, C. M., Johannes, M. S., Lopes, H. F., and Polson, N. G. (2010). Particle learning and smoothing. *Statistical Science* **25**, 88–106.

- Dukic, V., Lopes, H. F., and Polson, N. G. (2012). Tracking epidemics with Google Flu Trends data and a state-space SEIR model. *J. Am. Stat. Assoc.* **107**, 1410–1426.
- Durham, G. B. and Gallant, A. R. (2002). Numerical techniques for maximum likelihood estimation of continuous-time diffusion processes. *Journal of Business and Economic Statistics* **20**, 297–338.
- Elerian, O., Chib, S., and Shephard, N. (2001). Likelihood inference for discretely observed nonlinear diffusions. *Econometrica* **69**, 959–993.
- Elf, J. and Ehrenberg, M. (2003). Fast evaluation of fluctuations in biochemical networks with the linear noise approximation. *Genome Research* **12**, 2475–2484.
- Ferm, L., Lötstedt, P., and Hellander, A. (2008). A hierarchy of approximations of the master equation scaled by a size parameter. *J. Sci. Comput.* **34**, 127–151.
- Giagos, V. (2011). *Inference for autoregulatory genetic networks using diffusion process approximations*. PhD thesis, Lancaster University.
- Gillespie, D. T. (2005). A rigorous derivation of the chemical master equation. *Physica A* **188**, 404–425.
- Ginsberg, J., Mohebbi, M. H., Patel, R. S., Brammer, L., Smolinski, M. S., and Brilliant, L. (2009). Detecting influenza epidemics using search engine query data. *Nature* **457**, 0028–0836.
- Golightly, A. and Wilkinson, D. J. (2005). Bayesian inference for stochastic kinetic models using a diffusion approximation. *Biometrics* **61**, 781–788.
- Golightly, A. and Wilkinson, D. J. (2006). Bayesian sequential inference for nonlinear multivariate diffusions. *Stat. Comput.* **16**, 323–338.
- Golightly, A. and Wilkinson, D. J. (2008). Bayesian inference for nonlinear multivariate diffusion models observed with error. *Comput. Statist. Data Anal.* **52**, 1674–1693.
- Hairer, E. and Wanner, G. (1991). *Solving Ordinary Differential Equations II: Stiff and*

- Differential–Algebraic problems*. Springer–Verlag.
- Hayot, F. and Jayaprakash, C. (2004). The linear noise approximation for molecular fluctuations within cells. *Physical Biology* **1**, 205–210.
- Jewell, C. P., Keeling, M. J., and Roberts, G. O. (2009). Predicting undetected infections during the 2007 foot-and-mouth disease outbreak. *J. R. Soc. Interface* **6**, 1145–1151 (electronic).
- Jones, D. S., Plank, M. J., and Sleeman, B. D. (2010). *Differential equations and mathematical biology*. Chapman & Hall/CRC Mathematical and Computational Biology Series. Chapman & Hall/CRC, Boca Raton, FL.
- Kloeden, P. E. and Platen, E. (1992). *Numerical solution of stochastic differential equations*. Springer, New York.
- Komorowski, M., Finkenstadt, B., Harper, C. V., and Rand, D. A. (2009). Bayesian inference of biochemical kinetic parameters using the linear noise approximation. *BMC Bioinformatics* **10**, 343.
- Kurtz, T. G. (1970). Solutions of ordinary differential equations as limits of pure jump Markov processes. *J. Appl. Probability* **7**, 49–58.
- Kurtz, T. G. (1971). Limit theorems for sequences of jump Markov processes approximating ordinary differential processes. *J. Appl. Probability* **8**, 344–356.
- Petzold, L. (1983). Automatic selection of methods for solving stiff and nonstiff systems of ordinary differential equations. *SIAM Journal on Scientific and Statistical Computing* **4**, 136–148.
- Pitt, M. K. and Shephard, N. (1999). Filtering via simulation: auxiliary particle filters. *Journal of the American Statistical Association* **94**, 590–599.
- Proctor, C. J., Soti, C., Boys, R. J., Gillespie, C. S., Shanley, D. P., Wilkinson, D. J., and Kirkwood, T. B. L. (2005). Modelling the actions of chaperones and their role in ageing.

Mechanisms of ageing and development **126**, 119–131.

Ramsay, J. O., Hooker, G., Campbell, D., and Cao, J. (2007). Parameter estimation for differential equations: a generalized smoothing approach. *Journal of the Royal Statistical Society: Series B (Statistical Methodology)* **69**, 741–796.

Roberts, G. O. and Rosenthal, J. S. (2001). Optimal scaling for various metropolis-hastings algorithms. *Statistical Science* **16**, 351–367.

Roberts, G. O. and Stramer, O. (2001). On inference for partially observed nonlinear diffusion models using the Metropolis-Hastings algorithm. *Biometrika* **88**, 603–621.

Rue, H., Martino, S., and Chopin, N. (2009). Approximate Bayesian inference for latent Gaussian models by using integrated nested Laplace approximations (with discussion) . *Journal of the Royal Statistical Society, Series B* **71**, 319–392.

Sherlock, C., Fearnhead, P., and Roberts, G. O. (2010). The random walk Metropolis: linking theory and practice through a case study. *Statistical Science* **25**, 172–190.

Srensen, H. (2004). Parametric inference for diffusion processes observed at discrete points in time: a survey. *International Statistical Review* **72**, 337–354.

van Kampen, N. G. (1997). *Stochastic processes in physics and chemistry*. Elsevier, Amsterdam.

Vaswani, N. (2008). Particle filtering for large-dimensional state spaces with multimodal observation likelihoods. *Signal Processing, IEEE Transactions on* **56**, 4583–4597.

Wilkinson, D. J. (2006). *Stochastic modelling for systems biology*. Chapman & Hall/CRC Mathematical and Computational Biology Series. Chapman & Hall/CRC, Boca Raton, FL.

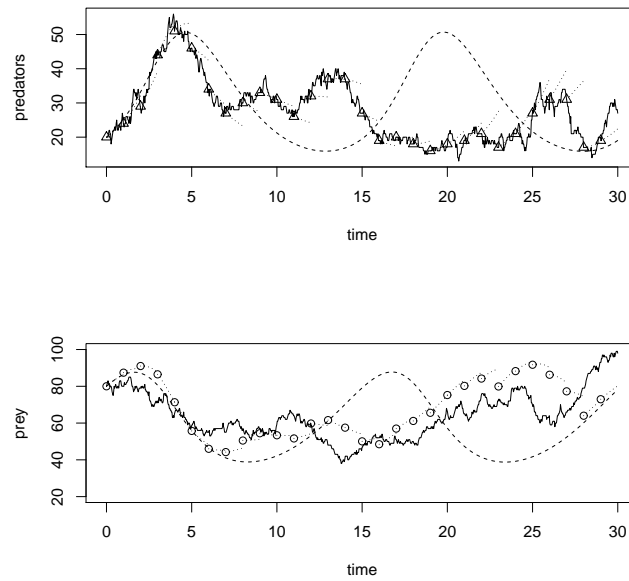


Figure 1. The true jump process (solid line) with observed values marked as triangles and posterior mean values at observation times marked as circles. The dashed line shows the LNA solution for the deterministic process integrated forward from the starting values, as used by Komorowski et al.; dotted lines show the LNA solution to the deterministic process integrated from the observed or posterior mean value at each observation time, as used in our LNA method. The top plot corresponds to predators (observed) the bottom plot to prey (unobserved).

Table 1

Comparison of our approach (LNA), the approach of Komorowski et al. (KOM) and the ODE approach (ODE). We present results in terms of the mean performance across 100 data sets.

	$\log_{10} \theta$	θ_1	θ_2	θ_3
		-2.000	-0.222	-0.523
Mean of posterior medians	LNA	-2.001	-0.248	-0.541
	KOM	-2.000	-0.263	-0.540
	ODE	-2.007	-0.308	-0.540
Mean abs. error of median	LNA	0.043	0.056	0.050
	KOM	0.074	0.086	0.070
	ODE	0.080	0.126	0.098
Mean width of 95% CI	LNA	0.193	0.188	0.198
	KOM	0.138	0.153	0.156
	ODE	0.141	0.158	0.194
Coverage of 95% CI	LNA	93	84	88
	KOM	51	54	55
	ODE	43	29	30

Table 2*Comparison of our LNA approach with that of the SDE-based method of Golightly and Wilkinson (2005).*

		θ_1	θ_2	θ_3	θ_4	θ_5	θ_6	θ_7	θ_8
	$\log_{10} \theta$	-1.000	-0.155	-0.456	-0.699	-1.000	-0.046	-0.523	-1.000
Mean of post. med.	LNA	-0.921	-0.092	-0.466	-0.687	-0.856	-0.076	-0.523	-0.974
	GW05	-0.975	-0.135	-0.445	-0.643	-0.972	0.036	-0.506	-0.941
Mean abs. err. of med.	LNA	0.147	0.139	0.093	0.090	0.197	0.183	0.082	0.107
	GW05	0.107	0.107	0.097	0.103	0.100	0.120	0.086	0.118
Mean width of 95% CI	LNA	0.730	0.721	0.408	0.410	1.065	1.047	0.410	0.429
	GW05	0.533	0.534	0.441	0.428	0.565	0.600	0.413	0.437
Coverage of 95% CI	LNA	94	94	89	92	94	95	92	88
	GW05	95	93	91	86	97	97	91	86
Mean ESS/sec	LNA	2.28	2.67	0.79	1.04	1.24	1.24	0.97	0.56
	GW05	0.18	0.18	0.60	1.10	0.09	0.08	0.68	0.82

Table 3

Accuracy of one-week-ahead predictions for New Zealand as a whole for the one- and two-compartment models using the LNA and for the one-compartment model using SMC; average bias and mean absolute deviation (in cases per 100,000) and mean width (also in cases per 100,000, denoted MWCI) and coverage of the 95% credibility interval.

Year	Method	Bias	MAD	MWCI	Cov.
2008	LNA2CM	-2.01	6.03	21.8	84
	LNA1CM	-1.11	5.96	29.1	84
	SMC1CM	-3.07	6.95	185.7	100
2009	LNA2CM	0.28	12.90	36.6	84
	LNA1CM	-0.27	14.72	40.51	86
	SMC1CM	-13.89	21.47	211.3	100
2010	LNA2	0.08	6.42	19.4	82
	LNA1CM	-0.37	6.29	21.6	84
	SMC1CM	-4.24	8.38	113.8	100
2011	LNA2CM	-0.83	5.09	18.3	84
	LNA1CM	-1.02	4.95	18.1	82
	SMC1CM	-1.50	5.82	92.2	100

Web-based Supplementary Materials for *Inference for reaction networks using the Linear Noise Approximation* by

Paul Fearnhead^{1,*}, Vasilios Giagos^{2,**}, and Chris Sherlock^{1,***}

¹Department of Mathematics and Statistics, Lancaster University, Lancaster, LA1 4YF, UK.

²School of Mathematics, Statistics and Actuarial Science, University of Kent, Canterbury, Kent CT2 7NF, UK.

**email:* p.fearnhead@lancaster.ac.uk

***email:* v.giagos@kent.ac.uk

****email:* c.sherlock@lancaster.ac.uk

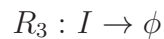
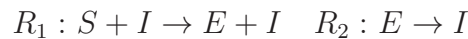
arXiv:1205.6920v2 [stat.ME] 4 Feb 2014

SomeDate

Appendix A: Epidemic Models

Example 3: An SEIR model

The SEIR epidemic model ([Anderson et al., 1992](#)) describes the evolution of an epidemic in a population. Each member of the population can be either susceptible, exposed, infected or removed. We denote the number of people in each of these states by S , E , I and ϕ respectively. The reactions for this model are



If we assume the population is randomly mixing, so that each person is equally likely to come into contact with any others, then the rates for these reactions will be $(\theta_1 SI, \theta_2 E, \theta_3 I)$.

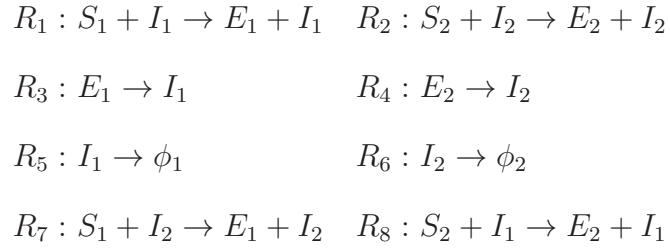
If we further assume a fixed population size then, as $S + E + I + \phi$ will remain constant, we can define the state of the process as being just the number of people that are susceptible, exposed and infected, (S, E, I) . The resulting net effect matrix is

$$\mathbf{A}' = \begin{bmatrix} -1 & 0 & 0 \\ 1 & -1 & 0 \\ 0 & 1 & -1 \end{bmatrix}$$

Example 4: A two-component SEIR model

Household models (e.g. [Andersson and Britton, 2000](#), Chapter 6) are used to model the spread of an infection which is transmitted at different rates between different pairs of individuals. In particular, infection spreads at a higher rate between individuals in the same household than it does between individuals in different households. We apply the same idea to the populations of two islands, say A_1 and A_2 , (rather than two households). The four

states for island i correspond to the number of susceptibles (S_i), exposed (E_i), infected (I_i) and removed (R_i) people who are resident on that island. The reactions for this model are



Since the behaviour of the inhabitants of each island A_i might well be different, and different with respect to each other island we allow for four different rates of transmission: between individuals who are resident in A_1 (θ_1), between individuals resident in A_2 (θ_2), from individuals resident in A_1 to those resident in A_2 (θ_6) and from individuals resident in A_2 to those resident in A_1 (θ_5). The reaction rates are therefore $(\theta_1 S_1 I_1, \theta_2 S_2 I_2, \theta_3 E_1, \theta_3 E_2, \theta_4 I_1, \theta_4 I_2, \theta_5 S_1 I_2, \theta_6 S_2 I_1)$.

Assuming a fixed population size for each island, means that we can reduce the dimension of the state-vector. Taking this to be $(S_1, E_1, I_1, S_2, E_2, I_2)$, the net-effect matrix is \mathbf{A} , where

$$\mathbf{A}' = \begin{bmatrix} -1 & 0 & 0 & 0 & 0 & 0 & -1 & 0 \\ 1 & 0 & -1 & 0 & 0 & 0 & 1 & 0 \\ 0 & 0 & 1 & 0 & -1 & 0 & 0 & 0 \\ 0 & -1 & 0 & 0 & 0 & 0 & 0 & -1 \\ 0 & 1 & 0 & -1 & 0 & 0 & 0 & 1 \\ 0 & 0 & 0 & 1 & 0 & -1 & 0 & 0 \end{bmatrix}$$

Appendix B: ODE solution for the LNA

Define $\mathbf{m}(t) := \mathbb{E} [\mathbf{M}(t)]$, $\mathbf{G}(t) := \mathbb{E} [\mathbf{M}(t)\mathbf{M}(t)^t]$ and $\mathbf{\Psi}(t) := \text{Var} [\mathbf{M}(t)] = \mathbf{G}(t) - \mathbf{m}(t)\mathbf{m}(t)^t$.

Then by the linearity of expectation and the fact that $d\mathbf{M}(t) = \mathbf{F}(t)\mathbf{M}(t) dt + \mathbf{S}(t) d\mathbf{W}(t)$,

$$\begin{aligned}
d\mathbf{m}(t) &= \mathbb{E} [d\mathbf{M}(t)] = \mathbb{E} [\mathbf{F}(t)\mathbf{M}(t) dt] = \mathbf{F}(t)\mathbf{m}(t) dt. \\
d\mathbf{G}(t) &= \mathbb{E} [\mathbf{M}(t+dt)\mathbf{M}(t+dt)^t - \mathbf{M}(t)\mathbf{M}(t)^t] \\
&= \mathbb{E} [\mathbf{M}(t)d\mathbf{M}(t)^t + d\mathbf{M}(t)\mathbf{M}(t)^t + d\mathbf{M}(t)d\mathbf{M}(t)^t] \\
&= \mathbb{E} [\mathbf{M}(t)\mathbf{M}(t)^t\mathbf{F}(t)^t + \mathbf{F}(t)\mathbf{M}(t)\mathbf{M}(t)^t] dt \\
&\quad + \mathbb{E} [\mathbf{S}(t)\mathbf{S}(t)^t] dt \\
&= \mathbf{G}(t)\mathbf{F}(t)^t + \mathbf{F}(t)\mathbf{G}(t) + \mathbf{S}(t)\mathbf{S}(t)^t. \\
d\mathbf{\Psi}(t) &= d\mathbf{G}(t) - \mathbf{m}(t) d\mathbf{m}(t)^t - d\mathbf{m}(t) \mathbf{m}(t)^t \\
&= \mathbf{\Psi}(t)\mathbf{F}(t)^t + \mathbf{F}(t)\mathbf{\Psi}(t) + \mathbf{S}(t)\mathbf{S}(t)^t,
\end{aligned}$$

as required.

Appendix C: Estimation of transition probabilities

The SDE and the LNA can be viewed as nested approximations to the evolution of the reaction network. The accuracy of the transition densities arising from these two approximations is now investigated for the autoregulatory model (Example 2). Both the LNA and the SDE arise from a continuous approximation to a discrete process, with the LNA also assuming that stochastic variations are small compared to the magnitude of the process itself, and we might therefore expect both approximations to improve as the system size increases. Three different system sizes are therefore compared with initial conditions $\mathbf{x}(0) = (5\Omega, 8\Omega, 8\Omega, 8\Omega, 5\Omega)$ for $\Omega \in \{1, 10, 100\}$.

The rate parameter vector was set to $\boldsymbol{\theta} = (0.1/\Omega, 0.7, 0.35, 0.2, 0.1/\Omega, 0.9, 0.3, 0.1)$ so as to keep the behaviour of the system (and of the drift ODE) consistent with the system examined

in [Golightly and Wilkinson \(2005\)](#), which uses the above initial state vector and rate vector with $\Omega = 1$. The true system was simulated forward 10000 times and the distribution of species was stored after $t_1 = 0.1$ time unit, $t_2 = 0.5$ time unit and $t_3 = 2.5$ time units. The SDE was integrated forward 10000 times using an Euler-Maruyama time step of 0.001 time units. Finally the parameters for the multivariate Gaussian transition density for t_1 , t_2 and t_3 were estimated by integrating forward the drift and variance ODEs.

[Figure 1 about here.]

Comparison of the transition parameters are shown in [Figure 1](#). The error induced by representing the true system with a continuous approximation can be seen for the small and medium system sizes. However, throughout both the LNA and SDE models give, by eye, a reasonable approximation to the true transition density and there appears to be little difference in the accuracy of the two approximations. The main difference is that the LNA always gives a Gaussian approximation, whereas the SDE transition density can be non-Gaussian. Graphs for the other species showed the same pattern and comparisons of bivariate distributions all showed good agreement. Qualitatively similar results have been observed for a variety of models and parameter values; see [Giagos \(2011\)](#).

Appendix D: additional tables from the simulation study for the autoregulatory model

[Table 1 about here.]

[Table 2 about here.]

Appendix E: priors and additional results for the GFT analysis

The priors for our rate parameters use the independent truncated Gaussian distributions employed in [Dukic et al. \(2012\)](#) with the same (Gaussian) mean as that paper but with the

standard deviation doubled to represent our uncertainty in the values of these parameters for communities as opposed to individuals. All four transmission rates $(\theta_1, \theta_2, \theta_5, \theta_6)$ have $\theta \sim N(1.5, 1)\mathbf{1}_{\{\theta > 0\}}$. The rates for changing from exposed to infected is $\theta_3 \sim N(2, 1)\mathbf{1}_{\{\theta_3 > 0\}}$ and the recovery rate is $\theta_4 \sim N(1, 1)\mathbf{1}_{\{\theta_4 > 0\}}$.

For island specific variables let $i = 1, 2$ correspond to N and S Islands respectively. Let N_i be the population of island i which is assumed fixed at $(3366100, 1038400)$ over the period examined.

We follow a similar format to [Dukic et al. \(2012\)](#) for all other parameters and quantities, and assign Gamma priors with a shape parameter of 1.1; these are relatively vague yet tail off to zero as the parameter or other quantity approaches zero.

We have the prior $C \sim Gam(1.1, 1.1/10)$. Then the initial number of susceptibles is independent for each island conditional on C :

$$S_i(0)|C \sim Gam(1.1, 1.1/\mu_i) \quad \text{where } \mu_i = N_i/(2C).$$

Subject to the constraint

$$\mathbf{1}_{\{S_1(0)C \leq N_1\}} \mathbf{1}_{\{S_2(0)C \leq N_2\}}.$$

The variance of the observations is independent for each island:

$$\sigma_i^2 \sim Gam(1.1, 1.1/V_i), \quad \text{where } V_i = \left(\frac{5N_i}{10^5}\right)^2.$$

The noise in the data (in cases per 10^5) for the year preceding our analysis appears to have a standard deviation of around 5 (we simply need an estimate of the order of magnitude for a sensible prior). The above transforms this to the variance on a pseudo observation of number of communities infected.

The initial state for island i is Gaussian (as required by our methodology) with

$$\mathbb{E}[X_i(0)] = \left[S_i(0), \frac{a_i N_i}{2 \times 10^5 C}, \frac{a_i N_i}{10^5 C} \right],$$

where a_i is the observed number of cases per 10^5 in the last week in January (i.e. the week

prior to the start of the data file). We use the fact that the exposure rate is believed to be about twice the infected rate. The variance matrix is diagonal with the following entries

$$\text{diag} \left[0, 10 \times \left(\frac{N_i}{10^5 C} \right)^2, 10 \times \left(\frac{N_i}{10^5 C} \right)^2 \right].$$

[Figure 2 about here.]

[Table 3 about here.]

Appendix F: the adaptive RWM algorithm used to fit the SEIR models

The adaptive RWM algorithm updates the variance and overall scaling of the random walk Metropolis proposal distribution according to the history of the Markov chain. It is very similar to the algorithm in [Sherlock et al. \(2010\)](#), except that adaptations to the scaling parameter are relative rather than absolute.

Let θ denote the current (p-dimensional) parameter vector and θ^* the proposed new parameter vector. To ensure that any variance matrix calculated from the history of the chain is non-singular, the algorithm proceeds with a fixed kernel ($\theta^* \sim N_p(\theta, \Sigma_0)$) until the number of proposals that have been accepted is at least $2p^2$.

At each subsequent iteration, i , the proposal is sampled from a mixture distribution

$$\theta^* \sim \begin{cases} N_p(\theta, \Sigma_0) & \text{w.p. } \beta \\ N_p(\theta, \lambda_i^2 \Sigma_i) & \text{w.p. } 1 - \beta \end{cases},$$

for some $\beta \in (0, 1)$ (we chose $\beta = 0.05$). Here Σ_i is the variance of the MCMC sample from θ up to and including iteration $i - 1$. The adaptive scaling parameter, λ_i is initialised to $\lambda_0 = 1/\sqrt{p}$ and is altered each time the adaptive proposal distribution $N_p(\theta, \lambda_i^2 \Sigma_i)$ is used, at which point the update depends upon whether or not the proposal, θ^* , was accepted:

$$\lambda_{i+1} = \begin{cases} \lambda_i (1 + 2.3\delta/\sqrt{n}) & \text{if } \theta^* \text{ was accepted} \\ \lambda_i (1 - 1\delta/\sqrt{n}) & \text{if } \theta^* \text{ was rejected} \end{cases}$$

Here $n \leq i - 2p^2$ is the number of adaptive proposals that have been used so far, and δ is a user parameter which we set to 0.1. The algorithm targets an acceptance rate of $1/3.3 \approx 0.3$.

References

- Anderson, R. M., May, R. M., and Anderson, B. (1992). *Infectious diseases of humans: dynamics and control*, volume 28. Wiley Online Library.
- Andersson, H. and Britton, T. (2000). *Stochastic epidemic models and their statistical analysis*, volume 4. Springer New York.
- Dukic, V., Lopes, H. F., and Polson, N. G. (2012). Tracking epidemics with Google Flu Trends data and a state-space SEIR model. *J. Am. Stat. Assoc.* **107**, 1410–1426.
- Giagos, V. (2011). *Inference for autoregulatory genetic networks using diffusion process approximations*. PhD thesis, Lancaster University.
- Golightly, A. and Wilkinson, D. J. (2005). Bayesian inference for stochastic kinetic models using a diffusion approximation. *Biometrics* **61**, 781–788.
- Sherlock, C., Fearnhead, P., and Roberts, G. O. (2010). The random walk Metropolis: linking theory and practice through a case study. *Statistical Science* **25**, 172–190.

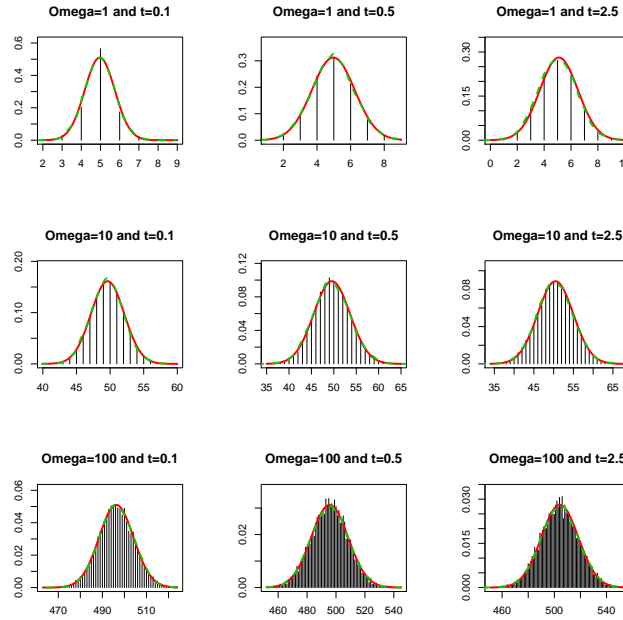


Figure 1. Transition probabilities for DNA (species 1) under rate vector $\theta = (0.1/\Omega, 0.7, 0.35, 0.2, 0.1/\Omega, 0.9, 0.3, 0.1)$ from an initial state of $(5\Omega, 8\Omega, 8\Omega, 8\Omega, 5\Omega)$ for $\Omega \in \{1, 10, 100\}$ estimated from the LNA (solid red line) and from 10000 simulations each for the true process (solid black bars) and the CLA (dashed green line) with an Euler timestep of $\Delta t = 0.001$. System sizes are $\Omega = 1$ (top row), $\Omega = 10$ (middle row) and $\Omega = 100$ (bottom row), and times are $t = 0.1$ (left column) $t = 0.5$ (middle column) and $t = 2.5$ (right column). For output from the exact simulation vertical bars are used to represent the relative probability of each outcome; kernel density estimates are used for the CLA, whilst for the LNA the plot simply shows the Gaussian density with the mean and variance estimated using the LNA. The y axis represents probability mass for the true process and probability density for the two continuous approximations. However x copies of a species simulated from the true process corresponds to between $x - 1/2$ and $x + 1/2$ copies using the continuous approximation. Since this interval has width 1 the probability mass and probability density plots are directly comparable.

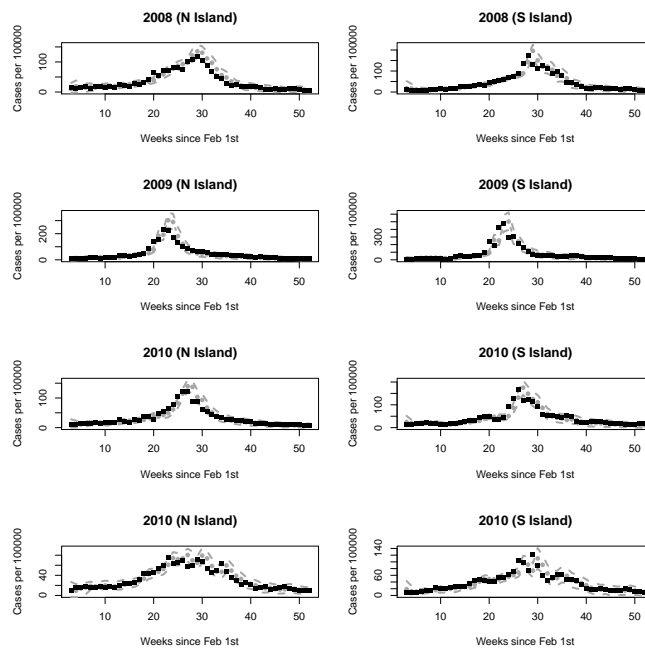


Figure 2. Observed influenza cases per 100000 from the GFT data for North and South Islands for 2008, 2009, 2010, and 2011 (black squares). Overlaid in grey are posterior median predictions using the LNA with a two-compartment SEIR model (circles and the central line) and upper and lower 95% credible bounds (dashed lines).

Table 1

Comparison of our LNA approach with that of the SDE-based method of Golightly and Wilkinson (2005). The true reaction rates are all four times larger than for

		<i>Table 2 in the main text</i>								
		$\log_{10} \theta$	θ_1	θ_2	θ_3	θ_4	θ_5	θ_6	θ_7	θ_8
Mean of post. med.	LNA	-0.592	0.229	-0.099	-0.324	-0.596	0.324	-0.164	-0.638	
	GW05	-0.674	0.160	0.180	-0.037	-0.804	0.219	0.090	-0.345	
Mean abs. err. of med.	LNA	0.216	0.235	0.257	0.233	0.205	0.236	0.252	0.246	
	GW05	0.276	0.287	0.110	0.086	0.407	0.337	0.102	0.091	
Mean width of 95% CI	LNA	1.258	1.263	0.559	0.669	1.359	1.356	0.564	0.716	
	GW05	0.500	0.502	0.490	0.350	0.460	0.500	0.458	0.360	
Coverage of 95% CI	LNA	100	100	59	79	99	99	59	75	
	GW05	40	40	90	90	0	5	93	91	

Table 2

Accuracy of our LNA approach on the auto-regulatory example. Results are for all components observed with Gaussian error (4GE) and three component observed either exactly (3NE) or with Gaussian error (3GE)

	$\log_{10} \theta$	θ_1	θ_2	θ_3	θ_4	θ_5	θ_6	θ_7	θ_8
		-1.000	-0.155	-0.456	-0.699	-1.000	-0.046	-0.523	-1.000
Mean of posterior medians	4GE	-0.860	-0.035	-0.439	-0.612	-0.842	0.086	-0.497	-0.905
	3NE	-0.737	-0.147	-0.320	-0.542	-0.843	0.088	-0.539	-0.821
	3GE	-0.623	-0.117	-0.279	-0.555	-0.833	0.093	-0.541	-0.833
Mean abs. error of median	4GE	0.211	0.202	0.153	0.195	0.207	0.192	0.143	0.212
	3NE	0.289	0.157	0.170	0.223	0.206	0.190	0.083	0.229
	3GE	0.395	0.142	0.205	0.234	0.217	0.201	0.158	0.239
Mean width of 95% CI	4GE	1.044	1.043	0.880	1.079	1.215	1.202	0.808	1.180
	3NE	1.340	1.187	0.829	1.154	1.217	1.202	0.422	1.128
	3GE	1.885	1.793	1.242	1.264	1.325	1.314	0.893	1.221
Coverage of 95% CI	4GE	93	93	97	95	96	98	96	91
	3NE	94	100	97	90	96	98	94	92
	3GE	100	100	96	96	97	99	97	95

Table 3

Accuracy of one-week-ahead predictions for New Zealand North and South Islands for the two-compartment model; average bias and mean absolute deviation (in cases per 100,000) and mean width (also in cases per 100,000, denoted MWCI) and coverage of the 95% credibility interval.

Year	Island	Bias	MAD	MWCI	Cov.
2008	N	-2.45	6.92	25.6	84
	S	-0.44	7.59	28.3	88
2009	N	0.16	12.56	38.0	90
	S	0.82	19.32	63.6	84
2010	N	-0.35	6.44	21.6	78
	S	1.50	9.14	29.7	80
2011	N	-1.23	5.40	20.7	90
	S	0.51	7.39	28.8	88